Powder Technology, 37 (1984) 25 - 37

FLUIDIZATION OF COHESIVE POWDERS

D.Geldart, N.Harnby and A.C.Wong
University of Bradford, School of Powder Technology,
United Kingdom

Abstract

Relatively small changes in particle size and other parameters which affect interparticle forces can transform a fine free-flowing powder into one which is cohesive. The influence of these parameters on the fluidization behaviour of fine powders has been investigated and can be readily assessed by measuring the ratio of tap to aerated bulk density.

Introduction

It has been known for more than 30 years that very fine particles are difficult to fluidize due to their cohesive properties. Interparticle forces have been a separate subject of study for many more years, but the first systematic study of interparticle forces in fluidized beds only appeared in 1966 [1]. It included fine particles which are naturally cohesive because of their small size as well as larger particles made artificially cohesive with additives.

The term "fine particles" is somewhat vague, and in his classification of powders into groups according to their fluidization behaviour, Geldart [2] distinguishes between free-flowing easy-to-fluidize group A powders and cohesive difficult-to-fluidize group C. A considerable amount of research has been devoted to group A powders largely because most commercial fluidized bed catalytic reactors use them; our basic scientific understanding of these powders has been advanced significantly by the research of Rietema and co-workers [3] and of Donsi, Massimilla and their co-workers [4], but the fluidization behaviour of group C powders has attracted much less attention [1,5]. Interest has increased recently [6,7,8] under the stimulation of commercial processes which wish to make use of them.

The interparticle forces in group A powders are small compared with the hydrodynamic forces acting within the fluidized bed and their influence is beneficial since they are responsible for the expanded dense phase which limits the growth of bubbles; for this reason group A powders should perhaps be called "slightly cohesive". In group C the interparticle forces are substantially larger than the hydrodynamic forces,

0032-5910/84/$3.00

the gas cannot readily separate particles and channelling occurs, giving poor fluidization. A better knowledge of the factors which influence the transition between groups A and C is of practical as well as scientific interest.

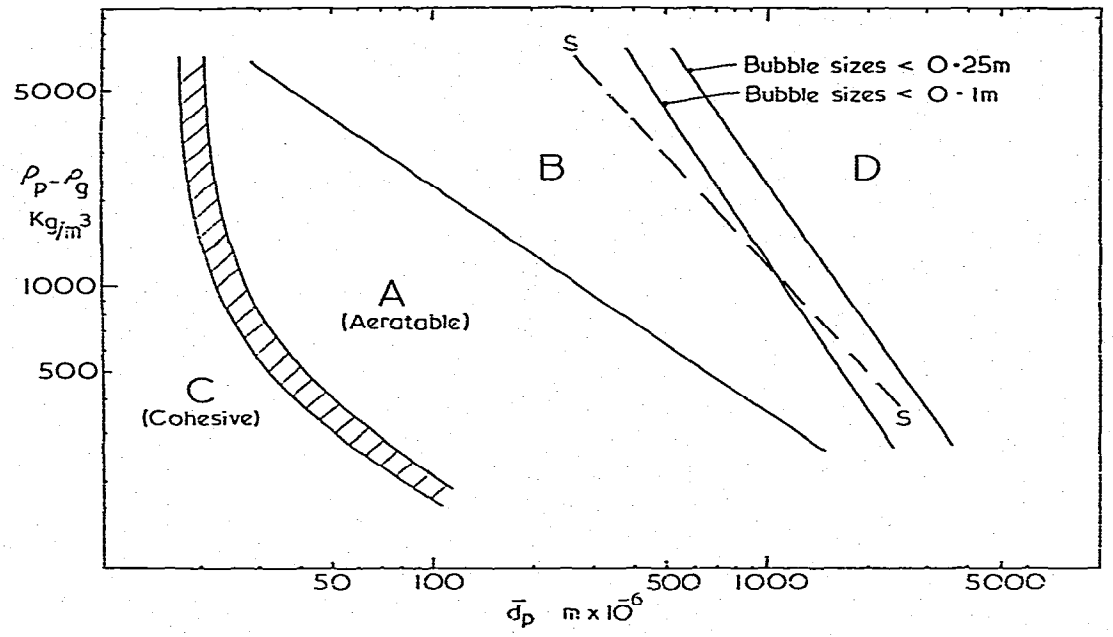

Figure 1 Powder classification diagram.

The work reported here forms part of a study financed by ICI PLC aimed at locating the group A/C borderline, and at understanding the extent to which the gas and particle characteristics influence the fluidization properties. In this paper we concentrate on some aspects of the fluidization behaviour of cohesive solids which appear to have gone unnoticed, or unreported, hitherto, and we compare and contrast them with the well-known behaviour of group A powders.

Choice of fluidization criteria and of powders and gases

The major differences between group A and B powders are summarised in table 1 and the most useful quantifiable criteria are the ratio U_{MB}/U_{MF}, the bed expansion ratio H/H_{MF}, and the bed deaeration rate. Since it is largely the interplay of hydrodynamic and interparticle forces which gives rise to these differences, we thought that measuring the same parameters in cohesive solids would be informative. We also decided to measure the rate of entrainment and the discharge rate through an orifice since both are of practical and scientific interest. Entrainment depends, inter alia, on bubbling behaviour as well as on particle interaction in the bed and freeboard.

In principle all the particle and gas properties shown in table 2 should be independent variables, but in practice one is limited to what is commercially available and can be modified cheaply so as to provide batches of several kilograms. High density solids tend to be

Table 1 *Summary of fluidization properties for powders in groups A and B*

	GROUP	
	A e.g. Cracking catalyst $\bar{d}_p \approx 60$ μm	B e.g. 75 μm < sand < 500 μm
U_{MB}/U_{MF}	> 1	≈ 1
Bed expansion	Considerable, goes through a minimum at 1<U<5 cm/s	Moderate, increases monotonically with U
Deaeration rate	Slow	Very fast
Other properties	Maximum bubble size, "fast" fluidization possible	No maximum bubble size, "fast" fluidization unlikely

Table 2 *Parameters influencing fluidization behaviour.*

INDEPENDENT VARIABLES	
Particle properties	Gas properties
Density, Size	Density
Size distribution	Viscosity
Shape, Hardness	Relative Humidity (%RH)
Surface roughness	
Porosity	
Total pressure Temperature	
DEPENDENT VARIABLES	
Van der Waals forces, capillary forces electrostatics, gas adsorption	

be hard, low density solids soft; as-received powders tend to have a normal distribution, separated fractions are usually skewed. It is therefore virtually impossible to vary only one particle characteristic at a time. Although we used more than 30 powders and size fractions, much of our work centred on the behaviour of two types of alumina, each available in several mean sizes, and some alumina size-blends: their properties are given in table 3.

Air having a range of controlled relative humidities was used for most experiments but dry argon, nitrogen and arcton-12 (dichlorofluoromethane) were also used.

Table 3 Properties of powders used in experimental programme

PWD. NO.	Powder		$\bar{d}_p$ (μm)	ρ_p (kgm^{-3})	ρ_{BA} (kgm^{-3})	ρ_{BT} (kgm^{-3})	$\frac{\rho_{BT}}{\rho_{BA}}$	Shape
1	α320-N	ALUMINAS	30.0	3970	1542	2032	1.318	Angular
2	α320-O		28.0	3970	1579	2006	1.270	"
3	α360		23.9	3970	1420	1961	1.381	"
4	A4		23.4	3970	1535	2048	1.334	"
5	α500		15.3	3970	1217	1830	1.504	"
6	FRF5		70.0	2430	1141	1364	1.195	Rounded
7	FRF20		12.0	2430	778	1276	1.640	"
8	FRF40		10.0	2430	665	1195	1.797	"
9	FRF85		5.0	2430	465	1005	2.161	"
10	FRF20/16		25.0	2430	990	1290	1.303	"
11	FRF20/70		55.0	2430	1075	1307	1.216	"
12	9G4		34.5	1810	1039	1201	1.156	"
13	I1	CRACKING CAT.	120.0	1542	912	1061	1.163	Spherical
14	C1		51.0	1117	590	715	1.212	"
15	E-CAT		33.0	1500	778	1006	1.293	"
16	E-CAT FINES		12.0	2370	715	1032	1.443	"
17	F2/5	FILLITES	77.4	418	352	352	1.000	Spherical
18	F0.3		78.7	364	202	204	1.001	"
19	F3/7		67.5	369	186	190	1.002	"
20	SG		125.0	638	440	443	1.007	"
21	F2/5/50		40.0	418	197	240	1.218	"
22	F2/5/50-63		55.0	418	217	242	1.115	"
23	IO	IRON OXIDE	28.0	5000	2053	3168	1.543	Angular
24	IO(+45)		60.0	5000	2547	2959	1.162	"
25	IO(-45)		20.0	5000	1819	2814	1.547	"
26	FRF5/45	BLENDS	90.0	2430	1165	1361	1.168	Rounded
27	5%FRF85		42.0	2430	1160	1382	1.191	"
28	10%FRF85		30.0	2430	1147	1427	1.244	"
29	30%FRF85		14.0	2430	997	1565	1.570	"
30	50%FRF85		9.0	2430	793	1400	1.765	"
31	CORVIC/M		29.7	1637	252	444	1.762	Angular
32	CORVIC/U		26.2	1637	274	587	2.142	"
33	B20		25.7	2782	1597	1820	1.140	Spherical

Equipment and experimental techniques

The measurements of U_{MF}, U_{MB}, ΔP and bed expansion were carried out in a 0.152 m diameter x 1 m tall perspex column with a 0.2 m tall steel bottom section. The distributor was made up of two layers of thick IBECO papers glued at the edges with "Copydex" adhesive, and supported by a perforated zinc plate to give a total pressure drop of about 650 mm H_2O at a superficial gas velocity of 0.01 ms^{-1}. Bed pressure drop was measured using a 1 m long stainless steel probe of 3 mm diameter and 1.6 mm nominal bore. This had a 1 mm diameter hole (covered with filter paper to prevent ingress of powder) 6 mm above the sealed lower end. The probe was inserted so that it touched the surface of the distributor and the other end was connected directly to a water or mercury manometer. In addition, a pressure tap in the wall of the bed 0.063 m above the distributor provided an alternative for bed pressure drop measurements. A transparent scale was stuck on the bed wall to provide direct bed expansion measurements. The same bed was used for the bed collapse experiment but with the additional arrangement of a solenoid valve which was positioned in the air line immediately before the bed inlet. This arrangement allowed the fluidizing gas supply to be interrupted virtually instantaneously.

The relative humidity of the fluidizing air was controlled by a simple humidification rig, which consisted of two columns, one filled with water and packed with raschig rings, and the other filled with silica gel.

A 0.08 m diameter glass column with a total height of about 2.6 m was erected for the elutriation test. For simplicity, vacuum cleaner bags were used to collect the carryover instead of using a cyclone. The presence and extent of electrostatic forces were measured by suspending an earthed copper rod above the bed. The greater the electrostatics, the greater the mass of solids adhering to the rod.

Results and discussion

Incipient fluidization and bubbling

One of the difficulties associated with fluidization of the very fine powders of group C characteristics is that the incipient fluidization velocities are so low (0.01 cm/s) that sintered porous plates cannot give the high pressure drop required for even fluidization, and distributors have to be made up from several layers of paper. Even so, it quickly became apparent that any meaningful measurement of U_{MF} became virtually impossible for cohesive powders because the bed pressure drop was non-reproducible; it varied with time due, probably, to the creation, destruction and re-formation of channels. As we fluidized the more cohesive powders we experienced increasing difficulty in deciding what was U_{MB}; even at velocities of several centimeters per second no clear bubbles could be identified. We therefore decided to ignore both U_{MB} and U_{MF}, and to concentrate rather on other reproducible measurements. Dry et al. [7] have also recently reported similar experiences.

Bed pressure drop deficiency

In a free-flowing group A powder, providing the distributor has an adequate pressure drop, the pressure drop across the fluidized bed is

within one or two per cent of the theoretical value; that is $\Delta P_{FL} A/W = 1$. It is well-known that the actual/theoretical pressure drop ratio decreases as powders become more cohesive and this effect can be seen in figure 2 where cohesiveness is increased by (a) decreasing particle size, and (b) increasing the relative humidity (%RH) of the fluidizing air.

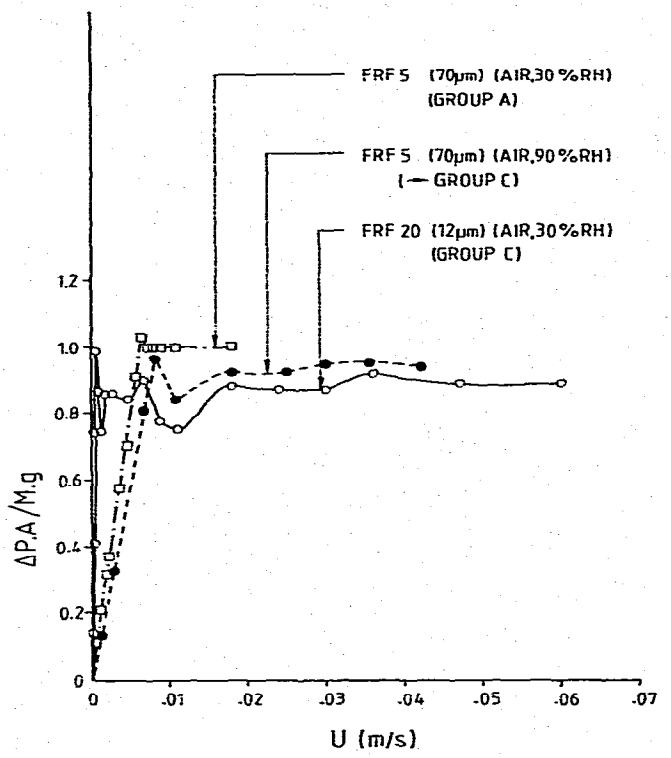

Figure 2 *Bed pressure drop – gas velocity curves showing effects of particle size and gas humidity.*

Bed expansion

There is a significant difference in the slope of the expansion curves of the two aluminas shown in figure 3. The reduction in the bed expansion observed just above U_{MB} with the group A powder occurs because the volume of the dense phase in the bubbling bed is reduced more rapidly than the bubble hold-up increases. This reduction in dense phase voidage is caused because the interparticle contacts are continually disrupted by the passage of bubbles and the consequent increase in overall powder circulation. In the more cohesive powder, the stronger interparticle forces allow the microvoids described by Massimilla and Donsì [9] to increase in number and/or size. Numerous horizontal and sloping cracks or channels form, and the bed expands without true bubble formation. Some small bubbles do form and although at the wall they can be seen to "wipe out" the cracks, the cracks reform with a different inclination and length. The addition to the bed of moisture in the form of air of high RH decreases bed expansion at low velocities but increases it at higher velocities. This too can be explained by

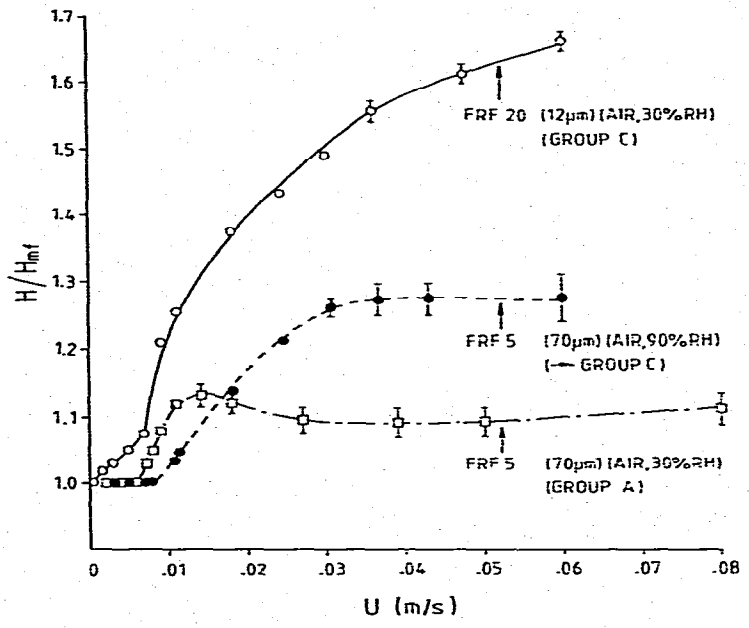

Figure 3 *Bed expansion – gas velocity curves showing effects of particle size and gas humidity.*

an increase in interparticle forces (in this case attributable to liquid bridges) which prevent the bed structure from expanding as much when the hydrodynamic drag forces are smaller (low velocities) but permit a higher voidage at higher velocities by giving the bed structure a greater mechanical strength. The data of d'Amore et al. [10] for glass particles support this explanation.

Bed collapse

Another striking difference between group A and C powders may be seen in the collapse or deaeration curves shown in figure 4. Ignoring the data for the first two seconds when the bubbles in the bed escape to the surface, the group A powder collapses at a constant rate. The cohesive powder collapses rapidly for the first 10 s. or so, and then at a gradually decreasing rate. The group C powder may remain in a slightly aerated state for a considerable period - many minutes or even several hours- with the pressure at the bottom of the bed decaying very slowly indeed.

The different bed structure in the two types of powder influences the way in which deaeration occurs. In the coarser alumina, the particles nearest the distributor quickly defluidize and assume a voidage close to that of a gently poured packed bed. The packed bed increases in thickness whilst the powder above it remains fluidized at a velocity similar to that in the dense phase in the bubbling bed. We suggest that in the cohesive powder, the gas in the cracks and microvoids adjacent to cracks leaves the bed rapidly, and the horizontal/sloping cracks cave-in giving rapid bed collapse. Subsequently the rate of collapse is controlled increasingly by the rate at which gas can escape

to a vertical channel from microvoids in the bulk of the powder. A group A powder made cohesive by moisture also gives a collapse curve having a similar shape to that of a group C powder.

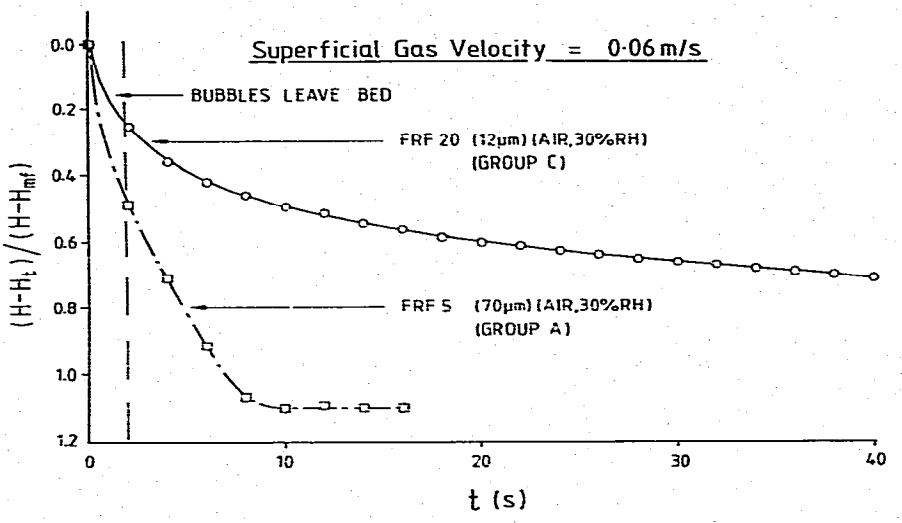

Figure 4 *Bed collapse curves for typical groups A and C powders.*

Flow out of an orifice

A 4 mm diameter hole with a rounded entrance was drilled in the side of the bed near the distributor and the mass discharge rate measured as a function of powder depth. The powders were maintained in an expanded, non-bubbling or gently bubbling condition (usually at $U \approx 1$ cm/s).

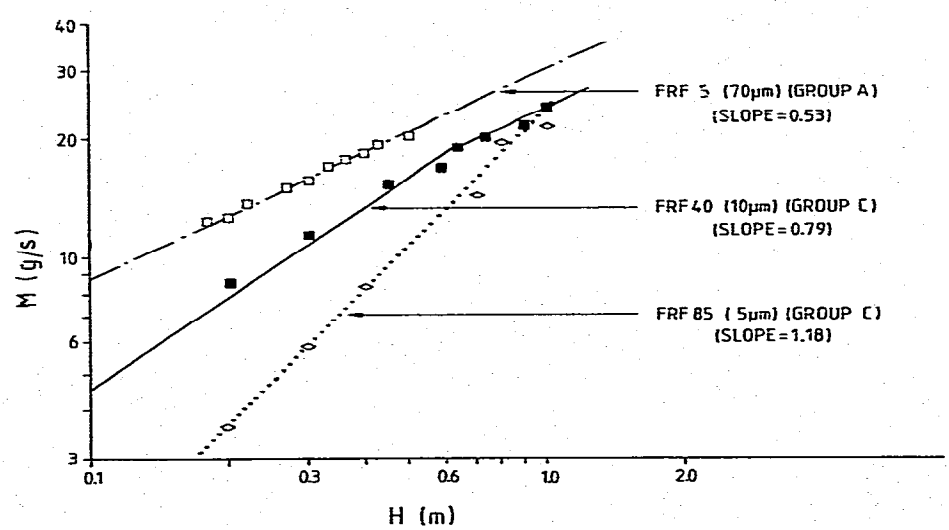

Figure 5 *Mass discharge rates through 4 mm diameter hole.*

The difference between the free-flowing 70 μm alumina and the two cohesive aluminas is quite striking (figure 5). The mass flow rate of free-flowing fluidized powders through orifices can be expressed as:

$$M = C_d \cdot \rho_{BMF} \frac{\pi}{4} (D_o - k\bar{d}_p) \sqrt[2]{2gh} \qquad (1)$$

where $k \approx 4$ and $0.4 < C_d < 0.7$ and H is the height of powder above the orifice.

The 70 μm alumina follows equation (1) in that the line has a slope of 0.5, but the cohesive aluminas deviate considerably. Their mass discharge rates at low bed heights are considerably below that of the coarse alumina but approach it for deeper beds. The data from the 10 μm alumina assumes a slope approaching 0.5 at H > 0.6 m though it is much steeper at low bed heights.

The pressure drop across a fluidized bed of cohesive solids can be up to 20% lower than theoretical but even after applying the appropriate corrections for this and also for the lower bulk densities of the finer powders, there is no difference in the slope of the lines. Our qualitative explanation is that the finer powders pass through the orifice in an agglomerated condition and have an effective particle size larger than the ultimate particle size. As the agglomerates move into the region near the orifice they are subject to shear stresses. These shear stresses will influence the size of the agglomerate - the larger the stress, the smaller the agglomerate. Calculations using equation (1), and assuming that there are no agglomerates at H = 1 m, gives effective particle sizes for the 5 μm powder ranging from 330 μm at H = 0.2 m down to 15 μm at H = 0.8 m.

Elutriation

Elutriation from fluidized beds is a complex affair and the mechanisms are not well understood even for free-flowing solids. They include the ejection of solids into the freeboard by bubbles, hydrodynamic interparticle effects (shielding), collisions and momentum interchange, agglomeration, and wall effects. Electrostatic effects can have an influence particularly on the batch elutriation of porous powders, and the %RH influences electrostatics by changing the conductivity of the air. It was therefore necessary to control %RH and to assess the electrostatics as described earlier.

It is generally assumed from the trend of elutriation data relating to group A and B solids (a) that as the average particle size of the bed decreases the elutriation rate, R_i, will increase, (b) that the elutriation rate of a sieve fraction increases as the size goes down, i.e. $R_i \propto 1/d_i^a$. However, from figure 6 it can clearly be seen that the fine cohesive alumina powders have significantly smaller carryover rates than the much coarser group A alumina. Increasing the %RH of the gas fluidizing a non-porous powder decreases the carryover, as shown in figure 7, and changes the shape of the curve.

It is not possible to say with absolute certainty whether it is the poorer fluidization in the bed which is responsible, though this does appear likely. It could be argued, as Yerushalmi and Cankurt [11] do, in the case of fast fluidisation, that considerable agglomeration

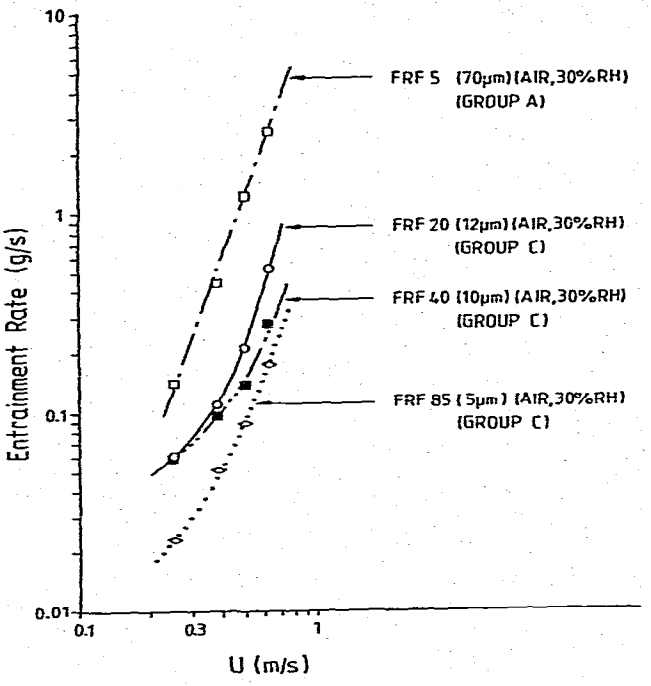

Figure 6 *Elutriation rate – gas velocity curves for groups A and C powders.*

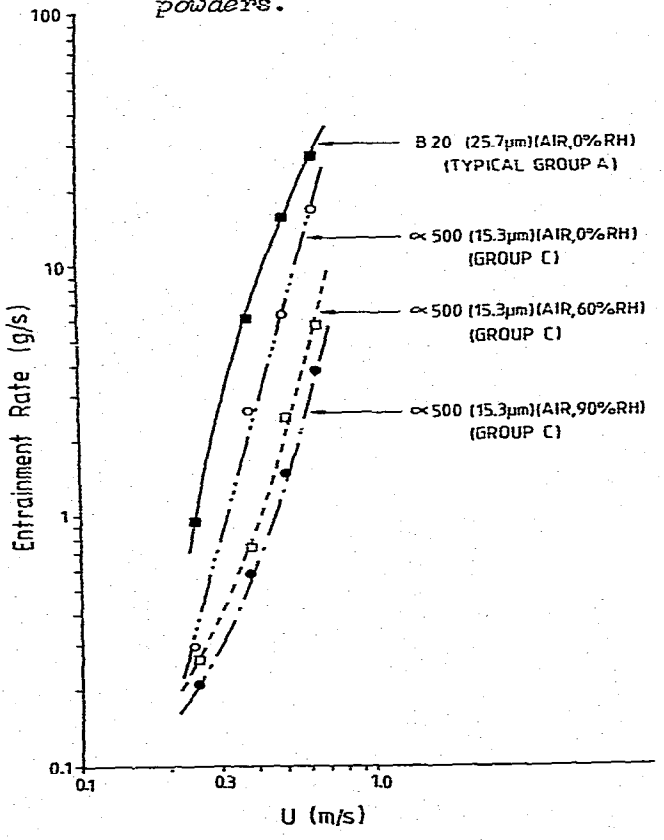

Figure 7

Elutriation rate – gas velocity curves showing effect of relative humidity

takes place in the freeboard giving a larger effective particle size; or that the more cohesive particles, on reaching the lower velocity region at the wall, agglomerate with each other and/or stick to the wall thus disengaging more effectively. As in many other aspects of fluidization, visual observation can teach us a great deal; we could clearly see that in the beds of cohesive solids far fewer bubble eruptions occurred, and when they did, agglomerates were ejected which disengaged in a short height. It is perhaps significant also that the shape of the elutriation curves for cohesive solids suggests that entrainment rates may approach those of group A powders at much higher velocities, when the high turbulence in the system would reduce agglomeration.

Ratio of tap to aerated bulk density

Our research programme included measurement of the internal angle of friction of the powders using a modified Jenike shear cell, behaviour of the powders in a rotating fluidized bed [12] and measurement of the vibrated and aerated bulk densities, ρ_{BT} and ρ_{BA}. Results of only the last are presented in this paper; the other results are available elsewhere [13]. The aerated density is obtained by pouring the powder through a vibrating sieve and allowing it to fall a fixed height into a cylindrical cup. The tapped density is then measured by causing the cylinder to fall 180 times through a known height whilst, at the same time, making powder additions to keep the cylinder full.

In a more extensive programme, in which the humidity was carefully controlled, and which will be reported fully elsewhere, it was found that although both ρ_{BT} and ρ_{BA} vary with RH, the ratio ρ_{BT}/ρ_{BA} (sometimes called the Hausner ratio) is virtually independent of %RH. This is rather convenient since it means that powders can be tested quickly under ambient conditions without the need to take special precautions. In figure 9, we have tried to draw together the observations from all 33 powders whose behaviour varied from very free flowing to very cohesive under dry conditions (%RH), as judged by the tests described earlier.

It is clear that there is a critical range for ρ_{BT}/ρ_{BA}. Powders having a ratio > 1.4 exhibit distinctly cohesive behaviour and should be considered as group C powders; a fine powder with a ratio less than 1.25 is certainly in group A, whilst those in the range 1.25 - 1.4 may exhibit some properties of both groups.

Conclusions

A study of the fluidization behaviour of fine powders (<70 μm) has revealed some striking differences between cohesive group C and free-flowing group A. In particular, when bed expansion and elutriation rates are plotted against gas velocity, and deaeration height is plotted against time, the two powder groups exhibit quite different characteristic curves. In addition, most group A powders can be made to behave like group C by fluidizing them with air of relative humidity in the range 60 - 90%.

A simple standardised test from which the tap density/aerated density can be obtained gives a good indication of the likely fluidization characteristics when the powder is fluidized by air of low humidity.

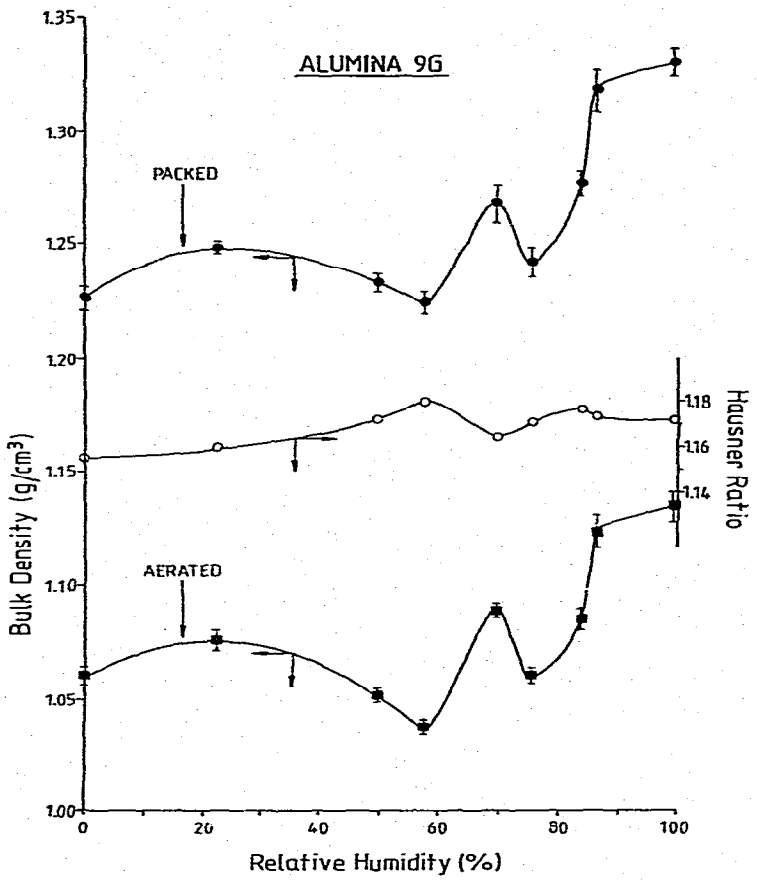

Figure 8

Aerated and tap densities as functions of relative humidity.

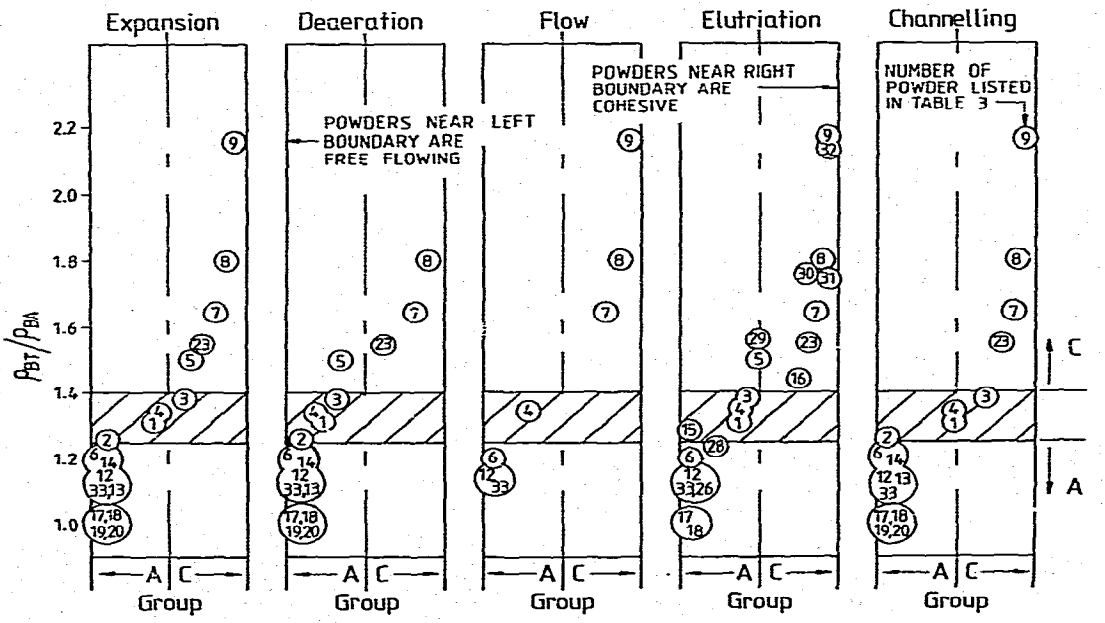

Figure 9 *Fluidization behaviour as functions of* ρ_{BT}/ρ_{BA}

References

1. Baerns M.: Ind. & Eng. Chem. Fund. 5, No.4, (1966) 508.
2. Geldart D.: Powder Tech. 7, (1973) 285.
3. Rietema K.: Proc. Int. Symp. Fluidization, Eindhoven, (1967) 154.
4. Donsi G. and Massimilla L.: Proc. Int. Symp. Fluidization and its Applications, Toulouse, (1973) 41.
5. Brekkan R.A., Lancaster E.B. and Wheelock T.D.: Chem.Eng.Symp.Ser. 66, (101), (1970) 81.
6. Nguyen C.T., Harnby N. and Burnet G.: Resource Recovery and Conservation 5, (1980) 255.
7. Dry R., Shingles T. and Judd M.R.: Powder Tech. (in press).
8. Staffin H.: Procedyne Inc. Private Communication (1981).
9. Massimilla L. and Donsi G.: Powder Tech. 15 (1976) 253.
10. D'Amore M., Donsi G. and Massimilla L.: Powder Tech. 23 (1979) 253.
11. Yerushalmi J. and Cankurt N.T.: Powder Tech. 24 (1979) 187.
12. Judd M.R. and Dixon P.D.: Trans. Inst. Chem. Engrs. 57 (1979) 67.
13. Wong A.C.: Ph.D.Dissertation, Univ. of Bradford (1983).

Notations

A	cross-sectional area of bed
C_d	discharge coefficient
D_o	diameter of hole
d_i	size of fraction
$\overline{d_p}$	mean size of powder
g	acceleration of gravity
H	height of fluidized bed
H_{MF}	height of bed at incipient fluidization
k	constant
M	mass flow rate of solids
R_i	rate of elutriation of fraction, size d_i
U	superficial gas velocity
U_{MB}	minimum bubbling velocity
U_{MF}	minimum fluidization velocity
W	weight of powder in bed
Δp	pressure drop across bed
Δp	pressure drop across fluidized bed
ρ_{BA}	aerated density of powder
ρ_{BT}	tap density of powder
ρ_{BMF}	bulk density of bed at minimum fluidization velocity